CARDIAC

MR 4D flow-based mean pulmonary arterial pressure tracking in pulmonary hypertension

Ursula Reiter[1] · Gabor Kovacs[2,3] · Clemens Reiter[1] · Corina Kräuter[1,4] · Volha Nizhnikava[1] · Michael Fuchsjäger[1] · Horst Olschewski[2,3] · Gert Reiter[1,5]

Abstract

Objectives Longitudinal hemodynamic follow-up is important in the management of pulmonary hypertension (PH). This study aimed to evaluate the potential of MR 4-dimensional (4D) flow imaging to predict changes in the mean pulmonary arterial pressure (mPAP) during serial investigations.

Methods Forty-four adult patients with PH or at risk of developing PH repeatedly underwent routine right heart catheterization (RHC) and near-term MR 4D flow imaging of the main pulmonary artery. The duration of vortical blood flow along the main pulmonary artery was evaluated from MR 4D velocity fields using prototype software and converted to an MR 4D flow imaging-based mPAP estimate ($mPAP_{MR}$) by a previously established model. The relationship of differences between RHC-derived baseline and follow-up mPAP values ($\Delta mPAP$) to corresponding differences in $mPAP_{MR}$ ($\Delta mPAP_{MR}$) was analyzed by means of regression and Bland-Altman analysis; the diagnostic performance of $\Delta mPAP_{MR}$ in predicting mPAP increases or decreases was investigated by ROC analysis.

Results Areas under the curve for the prediction of mPAP increases and decreases were 0.92 and 0.93, respectively. With the natural cutoff $\Delta mPAP_{MR} = 0$ mmHg, mPAP increases (decreases) were predicted with an accuracy, sensitivity, and specificity of 91% (91%), 85% (89%), and 94% (92%), respectively. For patients in whom 4D flow allowed a point estimate of mPAP (mPAP > 16 mmHg), $\Delta mPAP_{MR}$ correlated strongly with $\Delta mPAP$ ($r = 0.91$) and estimated $\Delta mPAP$ bias-free with a standard deviation of 5.1 mmHg.

Conclusions MR 4D flow imaging allows accurate non-invasive prediction and quantification of mPAP changes in adult patients with PH or at risk of developing PH.

Trial registration ClinicalTrials.gov identifier: NCT00575692 and NCT01725763

Key Points
• *MR 4D flow imaging allows accurate non-invasive prediction of mean pulmonary arterial pressure increases and decreases in adult patients with or at risk of developing pulmonary hypertension.*
• *In adult patients with mean pulmonary arterial pressure > 16 mmHg, MR 4D flow imaging allows estimation of longitudinal mean pulmonary arterial pressure changes without bias with a standard deviation of 5.1 mmHg.*

Keywords Pulmonary hypertension · Hemodynamics · Magnetic resonance imaging · Follow-up studies

Abbreviations

$\Delta mPAP$	Change in mPAP
$\Delta mPAP_{MR}$	Change in $mPAP_{MR}$
4D flow	Time-resolved, three-directional phase contrast imaging
4D	4-dimensional

✉ Ursula Reiter
ursula.reiter@medunigraz.at

1 Division of General Radiology, Department of Radiology, Medical University of Graz, Graz, Austria

2 Division of Pulmonology, Department of Internal Medicine, Medical University of Graz, Graz, Austria

3 Ludwig Boltzmann Institute for Lung Vascular Research Graz, Graz, Austria

4 Institute of Medical Engineering, Graz University of Technology, Graz, Austria

5 Research & Development, Siemens Healthcare Diagnostics GmbH, Graz, Austria

ANOVA	Analysis of variance
bSSFP	Balanced steady-state free precession
CTEPH	Chronic thromboembolic PH
ECG-gated	Electrocardiographically gated
EDV	End-diastolic volume
EF	Ejection fraction
ESV	End-systolic volume
GRAPPA	Generalized autocalibrating partial parallel acquisition
LV	Left ventricle
LVM	Left ventricular mass
mPAP	Mean pulmonary arterial pressure
$mPAP_{MR}$	4D flow-based mPAP estimate
MR	Magnetic resonance
MRI	Magnetic resonance imaging
PAH	Pulmonary arterial hypertension
PAWP	Pulmonary arterial wedge pressure
PH	Pulmonary hypertension
PVR	Pulmonary vascular resistance
RHC	Right heart catheterization
RV	Right ventricle
RVM	Right ventricular mass
RVOT	Right ventricular outflow tract
SV	Stroke volume
t_{vortex}	Duration of vortical blood flow along the pulmonary artery

Introduction

Pulmonary hypertension (PH) is a progressive, heterogeneous, potentially life-shortening pathophysiological condition diagnosed invasively by right heart catheterization (RHC) as a mean pulmonary arterial pressure (mPAP) exceeding 20 mmHg at rest [1]. The current guidelines recommend a multidimensional approach for PH treatment monitoring, including the evaluation of clinical, cardiopulmonary exercise, hematologic, and imaging parameters [2–6]. Serial assessment of the hemodynamic profile by RHC is recommended to guide therapy decisions particularly in case of clinical deterioration [2, 3].

Even though the role of cardiac MRI in the clinical management of PH is not yet established, the method offers various tools particularly suitable for PH treatment monitoring and patient follow-up. Allowing for an accurate evaluation of cardiac function and morphology, various quantitative MRI parameters have been reported to be significantly altered in PH [7–20] including, among others, the appearance of vortical blood flow along the main pulmonary artery as assessed by time-resolved, three-directional MR phase contrast (4D flow) imaging [19, 21–28]. Moreover, the duration of vortical blood flow was introduced as a potential 4D flow metric for accurate non-invasive estimation of elevated mPAP [26, 27],

making MR 4D flow imaging particularly interesting for non-invasive mPAP tracking. Although there are sparse reports of cases featuring changes in the appearance of vortical blood flow patterns in chronic thromboembolic PH after percutaneous transluminal pulmonary angioplasty [29] and pulmonary thromboendarterectomy [30], it remains unknown whether the observed pressure relationship of vortical blood flow in the main pulmonary artery persists during PH therapy and whether differences in the duration of vortical blood flow along the main pulmonary artery can predict mPAP changes during treatment.

The purpose of the present study was therefore to compare MR 4D flow imaging and RHC-derived mPAP differences from serial investigations of patients with PH or at risk of developing PH and to analyze the potential of MR 4D flow to non-invasively predict mPAP changes during the clinical workup of such patients.

Materials and methods

Study population

Forty-four subjects with PH or at risk of developing PH (including patients with connective tissue diseases, interstitial lung disease, and portal hypertension), who underwent baseline and follow-up RHC and MR 4D flow imaging at 1.5 T or 3 T between August 2006 and November 2016, were retrospectively enrolled from two prospective studies in which consecutive patients scheduled for routine RHC were also scheduled for near-term comprehensive cardiac MRI (ClinicalTrials.gov identifier NCT00575692 and NCT01725763). The studies complied with the Declaration of Helsinki and were approved by the local ethics review board. Written informed consent was obtained from all participants. Baseline RHC and corresponding cardiac MRI were performed within 8 ± 13 days of each other. Follow-up RHC and cardiac MRI were performed within 8 ± 21 days of each other, 824 ± 839 days from the baseline investigation. No clinically relevant changes in drug treatment or disease state occurred between RHC and the corresponding cardiac MRI.

Right heart catheterization

RHC was performed with a 7-French quadruple lumen, balloon-tipped, flow-directed Swan-Ganz catheter (Baxter Healthcare Corp.) using the transjugular approach with the patient positioned supine. RHC parameters assessed included mPAP to diagnose PH, as well as the mean pulmonary artery wedge pressure (PAWP), cardiac output (CO), and the pulmonary vascular resistance (PVR), which were used for the clinical classification of PH patients.

Cardiac magnetic resonance imaging

Cardiac MRI was performed at 1.5 T (Magnetom Sonata, Siemens Healthcare) or 3 T (Magnetom Trio or Magnetom Skyra, Siemens Healthcare) with the patient in the supine position using phased-array body and spine matrix coils. In detail, for 19 patients, baseline and follow-up MRI investigations were performed at 1.5 T; for 16 patients, baseline and follow-up MRI investigations were performed at 3 T; and for 9 patients, baseline investigations at 1.5 T were followed-up by 3 T MRI.

The cardiac MRI protocol included assessment of retrospectively electrocardiographically gated (ECG-gated), two-dimensional, segmented or ECG-gated, real-time cine balanced steady-state free precession (bSSFP) imaging, covering the entire left (LV) and right (RV) ventricles by a stack of contiguous slices in short-axis orientation. 4D flow data were acquired during free breathing in right ventricular outflow tract (RVOT) orientation, covering the main pulmonary artery with gapless slices of a retrospectively ECG-gated, two-dimensional, segmented, spoiled gradient-echo-based cine phase contrast sequence with three-directional velocity encoding. Velocity encoding was set to 90 cm/s in all directions and adapted if necessary to prevent aliasing. Table 1 provides a summary of 1.5T and 3T cine bSSFP and 4D flow protocol parameters.

Image analysis

LV and RV volumetric function parameters were evaluated from manual segmentation of end-diastolic and end-systolic LV/RV endocardial and epicardial borders in short-axis images using the Argus software (Siemens Healthcare). Myocardial trabeculations and papillary muscles were excluded from the LV and RV cavities. Volumetric function parameters assessed included end-diastolic (EDV) and end-systolic (ESV) volumes, stroke volume (SV), ejection fraction (EF), and LV/RV myocardial mass (LVM, RVM).

Baseline and follow-up 4D flow data of the main pulmonary artery were jointly evaluated using a prototype software (4D Flow, Siemens Healthcare) [28, 31]. After cropping spatially aliased structures, background phase correction was applied to all datasets. Blood flow patterns in the main pulmonary artery were analyzed with respect to the existence of vortical blood flow in consensus by two experienced readers (18 years of experience) using multiplanar reconstructed 3-dimensional vector fields in RVOT orientation (Fig. 1) and streamline representations. The duration of vortical blood flow along the main pulmonary artery (t_{vortex}) was defined as the percentage of cardiac phases with vortical blood flow in the cardiac interval as previously described [27, 28]. 4D flow-based mPAP ($mPAP_{MR}$) was calculated from t_{vortex} using the piecewise linear model previously given in Reiter et al [27]:

$$mPAP_{MR} \text{ (in mmHg)} \quad \begin{array}{ll} \leq 16 & \text{for } t_{vortex} = 0 \\ = 16 + 0.63 \cdot t_{vortex} & \text{for } t_{vortex} > 0 \end{array}$$

$$(1)$$

Changes in mPAP and $mPAP_{MR}$ were calculated as the differences between follow-up and baseline values and are denoted by $\Delta mPAP$ and $\Delta mPAP_{MR}$. An increase (decrease) in mPAP was defined as $\Delta mPAP > 0$ ($\Delta mPAP < 0$) together with the condition mPAP > 16 mmHg at follow-up (mPAP

Table 1 Sequence parameters of the cine bSSFP and 4D flow imaging protocols at 1.5 T and 3 T. Typical scan times for cine bSSFP protocols are given for the stack of contiguous slices in short-axis orientation; the typical scan times for 4D flow protocols are given for the stack of slices covering the main pulmonary artery. *GRAPPA*, generalized auto calibrating partial parallel acquisition; *Not applicable due to prospective ECG-gating

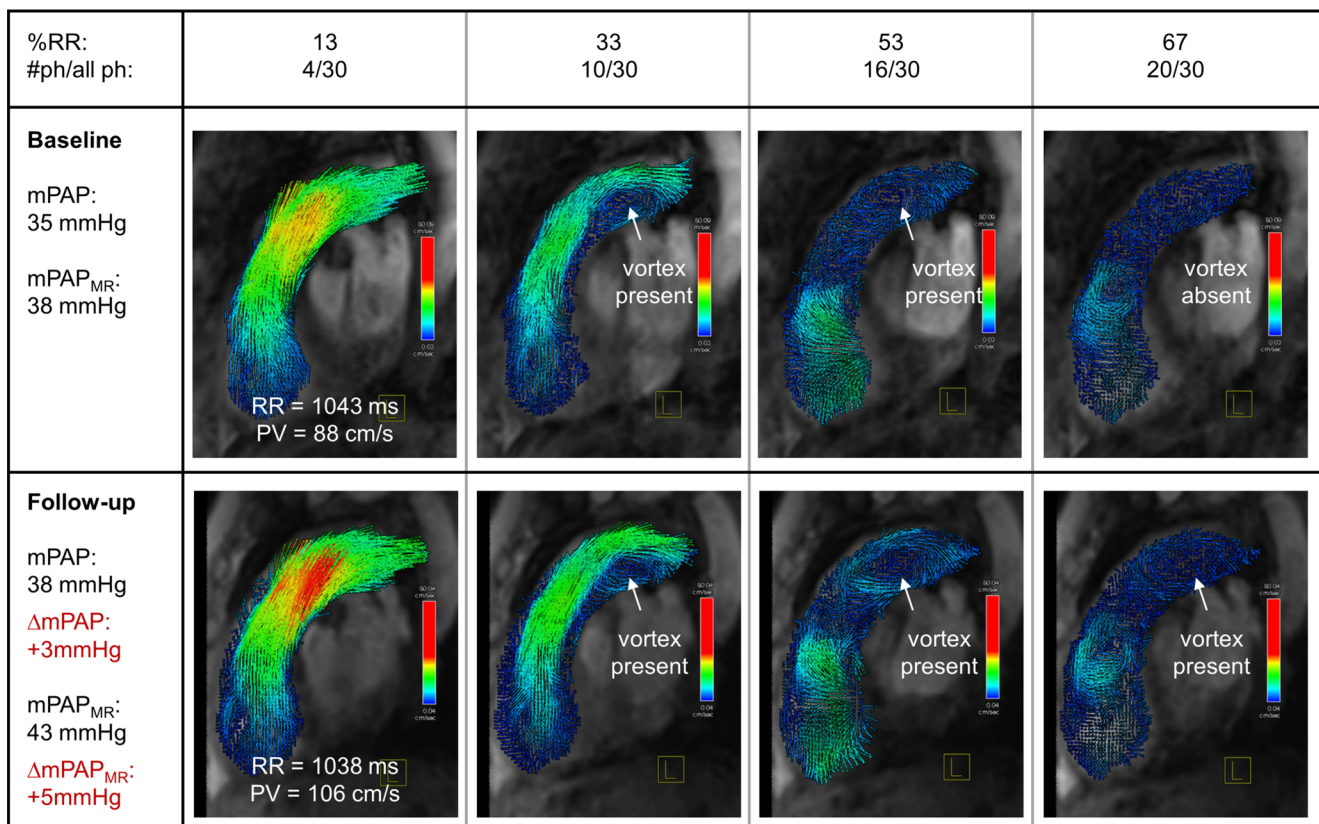| Parameters	Cine bSSFP		4D flow	
	Segmented @1.5 T	Real time @3 T	@1.5 T	@3 T
Measured in-plane resolution (mm²)	2.2 × 1.4	3.9–4.5 × 2.5–2.8	2.4 × 1.8	2.4 × 1.8
Slice thickness (mm)	8.0	8.0	6.0	4.0
Echo time (ms)	1.2	1.0–1.1	4.1	3.1
Echo spacing (ms)	2.8	2.3–2.5	7.4	5.2–5.9
Flip angle (°)	60	35–60	15	12–15
Measured temporal resolution (ms)	48–54	34–52	89	42–47
Number of reconstructed cardiac phases	30	–*	20	25–30
Bandwidth (Hz/pixel)	930	1240–1502	455	606
Parallel acquisition factor (using GRAPPA)	–	3	2	2
Averaging	1	1	3	2
Imaging time per slice (heartbeats)	7–8	1	57–78	40–60
Typical scan time (min)	4	< 1	8	8

Fig. 1 Velocity color-encoded 3-dimensional vector representation of vortical blood flow along the main pulmonary artery in a patient with PH at baseline (upper panel) and 2-year follow-up (lower panel). Color encoding of both representations was set to an equal scale. %RR, percentage of the cardiac interval; #ph, cardiac phase in the RR interval; (Δ)mPAP, mean pulmonary arterial pressure (difference) measured by right heart catheterization; (Δ)mPAP$_{MR}$, mean pulmonary arterial pressure (difference) estimated by 4D flow; PV, main pulmonary artery peak velocity magnitude. mPAP differences are written in red

> 16 mmHg at baseline) to enable the comparison with respective increases (decreases) in ΔmPAP$_{MR}$ in the entire study population, where, due to the absence of vortical blood flow for mPAP $\leq$ 16 mmHg, $t_{vortex} = 0$ allows only an interval-estimate of ΔmPAP$_{MR}$.

Statistical analysis

Mean values are given together with standard deviations; sensitivities and specificities are specified together with 95% confidence intervals in parentheses. Statistical analysis was performed using NCSS (Hintze, J. (2008) NCSS, LLC.). For statistical tests, a significance level of 0.05 was employed.

Differences in mean parameter changes from zero between baseline and follow-up investigations were analyzed by one-sample t test; relationships of parameter changes to ΔmPAP were analyzed by correlation analysis. The relationships between mPAP and mPAP$_{MR}$ as well as ΔmPAP and ΔmPAP$_{MR}$ were investigated by means of regression and Bland-Altman analysis. Dependencies of biases on MR field strength were analyzed by unpaired t test or analysis of variance (ANOVA) of three groups (baseline and follow-up at 1.5 T, baseline and follow-up at 3 T, baseline at 1.5 T and follow-up at 3 T). The diagnostic performance of mPAP$_{MR}$ in predicting PH and the diagnostic performance of ΔmPAP$_{MR}$ in predicting increases or decreases of mPAP were analyzed by receiver operating characteristic (ROC) curve analysis. Optimal cutoffs were defined as those that maximized the sum of sensitivity and specificity, whereas mPAP$_{MR}$ = 20 mmHg for diagnosing PH and ΔmPAP$_{MR}$ = 0 mmHg for diagnosing increases or decreases of mPAP were termed "natural cutoffs" due to the analogy to mPAP-definitions in RHC.

Results

Study population

At baseline, PH was diagnosed by RHC in 28 of 44 patients: 16 subjects were classified as having PH due to pulmonary arterial hypertension (PAH), 2 subjects as having PH due to lung diseases, 7 subjects as having chronic thromboembolic PH (CTEPH), and 3 subjects as having PH secondary to multifactorial mechanisms. At follow-up, one patient without PH at baseline developed PAH, and one patient with CTEPH at baseline revealed normal mPAP after surgical treatment.
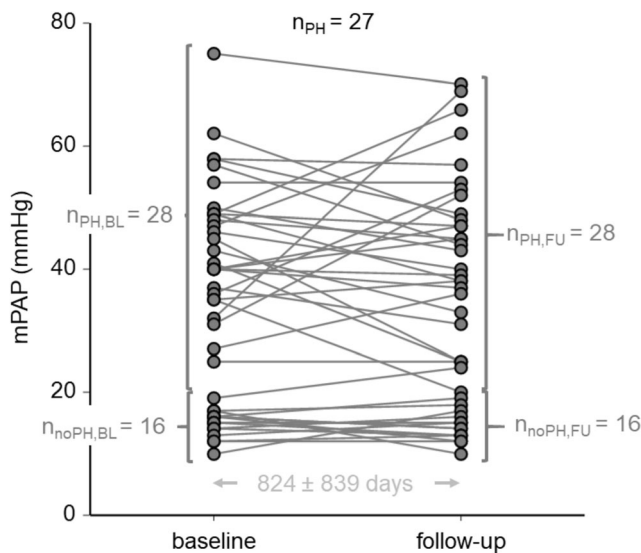
Fig. 2 Distributions of mPAP at baseline and at follow-up as well as the mPAP changes of the study population. $n_{PH,BL}$, number of subjects with PH at baseline; $n_{noPH,BL}$, number of subjects without PH at baseline; $n_{PH,FU}$, number of subjects with PH at follow-up; $n_{noPH,FU}$, number of subjects without PH at follow-up; n_{PH}, number of subjects with PH at baseline and follow-up

Consequently, PH was diagnosed in 28 patients at follow-up. mPAP > 16 mmHg was found in 31 patients at baseline, in 32 patients at follow-up, and mPAP > 16 mmHg was present in 30 patients at baseline and follow-up. Figure 2 illustrates the distributions of mPAP at baseline and at follow-up as well as

the mPAP changes of the study population. The demographic and hemodynamic characterization of the study population is summarized in Table 2 together with LV and RV volumetric function parameters at baseline and follow-up.

MR 4D flow-based prediction of PH and mPAP increase/decrease

Using $mPAP_{MR}$ to predict PH, the area under the curve (AUC) was 1.00 at both baseline and follow-up. At baseline, optimal and natural cutoff coincided, such that the cutoff of $mPAP_{MR}$ = 20 mmHg resulted in an accuracy of 100% (92–100%), a sensitivity of 100% (88–100%), and a specificity of 100% (79–100%) for diagnosing PH. At follow-up, the optimal (23 mmHg) and natural cutoffs did not coincide; the cutoff of $mPAP_{MR}$ = 20 mmHg resulted in an accuracy of 95% (84–99%), a sensitivity of 100% (88–100%), and a specificity of 88% (62–98%) for diagnosing PH.

AUCs for the prediction of increase or decrease of mPAP between baseline and follow-up based on $\Delta mPAP_{MR}$ were 0.92 (0.74–0.96) and 0.93 (0.75–0.98), respectively (Fig. 3a, b). In both cases, the optimal and natural ($\Delta mPAP_{MR}$ = 0 mmHg) cutoffs coincided. The accuracy, sensitivity, and specificity for predicting mPAP increase were 91% (78–97%), 85% (56–98%), and 94% (79–99%), respectively, while the corresponding values for predicting mPAP decrease

Table 2 Summary of demographic, right heart catheterization (RHC), and cardiac MR imaging parameters of the study population at baseline and follow-up, together with differences in parameters between baseline and follow-up, and the correlations of differences with mPAP changes ($r_{\Delta mPAP}$). Significant differences from 0 are indicated by *, significant correlations by +. n, number of subjects at baseline and follow-up; n_{PH}, number of subjects with PH at baseline and follow-up; n_{non-PH}, number of subjects without PH at baseline and follow-up

Parameter	All ($n = 44$)				PH ($n_{PH} = 27$)				Non-PH ($n_{non-PH} = 15$)		
	Base	FU	Diff	$r_{\Delta mPAP}$	Base	FU	Diff	$r_{\Delta mPAP}$	Base	FU	Diff
F/M (nr)	26/18	26/18			12/15	12/15			13/2	13/2	
Age (years)	59 ± 13	61 ± 13	2 ± 2*		60 ± 14	63 ± 14	2 ± 2*		57 ± 11	59 ± 11	2 ± 2*
Height (cm)	169 ± 9	169 ± 9	0 ± 3		171 ± 8	170 ± 9	0 ± 2		166 ± 10	166 ± 10	0 ± 3
Weight (kg)	76 ± 13	76 ± 13	0 ± 6		78 ± 12	79 ± 12	1 ± 6		71 ± 15	72 ± 15	0 ± 2
RHC											
mPAP (mmHg)	34 ± 17	34 ± 18	0 ± 10		45 ± 11	45 ± 13	0 ± 13		15 ± 2	14 ± 2	0 ± 3
PAWP (mmHg)	8 ± 3	9 ± 4	0 ± 4	0.31	9 ± 3	9 ± 5	0 ± 5	0.28	7 ± 2	7 ± 2	0 ± 3
PVR (WU)	6.1 ± 4.4	5.4 ± 4.3	- 0.7 ± 2.8	0.75+	8.7 ± 3.4	7.7 ± 3.4	- 1.0 ± 3.4	0.77+	1.5 ± 0.8	1.5 ± 0.5	0.0 ± 0.6
CO (l/min)	4.9 ± 1.8	5.1 ± 1.3	0.1 ± 1.6	- 0.07	4.4 ± 1.1	5.0 ± 1.3	0.7 ± 1.0*	- 0.16	6.1 ± 2.3	5.3 ± 1.1	- 0.8 ± 2.2
Cardiac MR imaging											
LVEDV (ml)	120 ± 33	124 ± 36	4 ± 30	- 0.19	122 ± 40	127 ± 42	5 ± 35	- 0.34	113 ± 17	118 ± 20	5 ± 21
LVESV (ml)	42 ± 23	43 ± 20	0 ± 18	0.01	45 ± 29	44 ± 25	-1 ± 20	- 0.05	37 ± 9	41 ± 11	4 ± 14
LVSV (ml)	78 ± 21	81 ± 24	3 ± 20	- 0.30+	77 ± 25	83 ± 28	6 ± 23	- 0.47+	77 ± 14	77 ± 12	0 ± 11
LVEF (%)	66 ± 11	66 ± 10	1 ± 9	- 0.17	64 ± 13	67 ± 12	2 ± 9	- 0.22	68 ± 5	66 ± 5	- 2 ± 8
LVM (g)	99 ± 26	104 ± 29	5 ± 23	- 0.09	102 ± 27	110 ± 29	8 ± 20*	- 0.09	96 ± 26	96 ± 27	0 ± 29
RVEDV (ml)	183 ± 88	194 ± 93	- 11 ± 54	0.32+	214 ± 88	236 ± 96	22 ± 49*	0.22	119 ± 22	125 ± 24	6 ± 24
RVESV (ml)	112 ± 81	111 ± 80	- 1 ± 38	0.61+	140 ± 86	140 ± 90	0 ± 37	0.67+	54 ± 14	62 ± 19	8 ± 22
RVSV (ml)	71 ± 22	84 ± 32	12 ± 33*	- 0.19	74 ± 23	96 ± 34	22 ± 34*	- 0.40+	64 ± 17	63 ± 12	- 2 ± 18
RVEF (%)	43 ± 15	47 ± 14	4 ± 14	- 0.45+	38 ± 15	44 ± 15	6 ± 13*	- 0.69+	54 ± 9	51 ± 9	- 2 ± 14
RVM (g)	80 ± 49	84 ± 49	5 ± 24	0.31+	99 ± 50	109 ± 47	10 ± 25*	0.23	43 ± 11	43 ± 9	0 ± 8

were 91% (78–97%), 89% (65–99%), and 92% (75–99%), respectively.

Restricting the study population to PH patients, the AUC values for the prediction of increase or decrease of mPAP were 0.94 (0.77–0.99) and 0.94 (0.76–0.98), respectively. The natural cutoff $\Delta mPAP_{MR} = 0$ mmHg resulted in an accuracy of 89% (72–98%), sensitivity of 90% (56–100%), and specificity of 89% (65–99%) for predicting mPAP increase, and an accuracy of 86% (67–96%), sensitivity of 88% (64–99%), and specificity of 82% (48–98%) for predicting mPAP decrease (Fig. 3c, d).

MR 4D flow-based assessment of mPAP and ΔmPAP

The correlation between mPAP and $mPAP_{MR}$ for patients with mPAP > 16 mmHg was strong at both baseline ($r = 0.95$) and follow-up ($r = 0.97$). Bias to RHC as the reference method was not found at either baseline or follow-up (0.2 mmHg, $p = 0.83$ and - 0.1 mmHg, $p = 0.90$ for baseline and follow-up, respectively). Standard deviations of differences were 4.0 mmHg for the baseline and 3.6 mmHg for the follow-up investigation (Fig. 4). Differences between mPAP and $mPAP_{MR}$ did not depend significantly on field strength ($p = 0.73$ for the baseline and $p = 0.19$ for the follow-up investigation).

In patients with mPAP > 16 mmHg at baseline and follow-up, $\Delta mPAP$ correlated strongly with $\Delta mPAP_{MR}$ ($r = 0.91$). There was no significant bias (- 0.3 mmHg, $p = 0.71$), and the standard deviation of differences was 5.1 mmHg (Fig. 5). The differences between $\Delta mPAP$ and $\Delta mPAP_{MR}$ did not depend significantly on field strength(s) used at baseline and follow-up ($p = 0.07$).

Discussion

The most important finding of this study is that MR 4D flow imaging of the main pulmonary artery during PH treatment
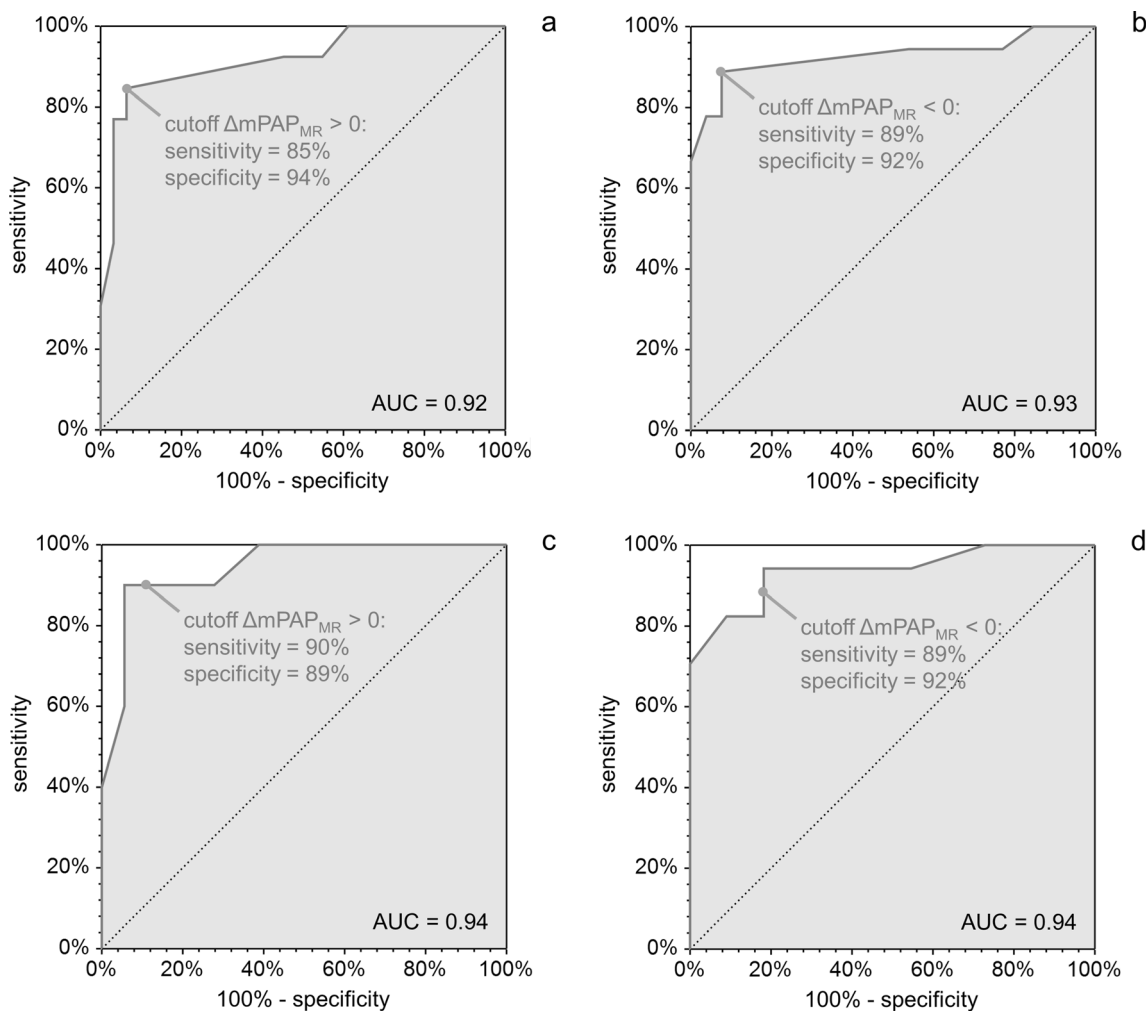
Fig. 3 ROC curves for the prediction of mPAP increase (**a**) and decrease (**b**) based on $\Delta mPAP_{MR}$ for the entire study population, as well as for mPAP increase (**c**) and decrease (**d**) for patients with PH at baseline RHC
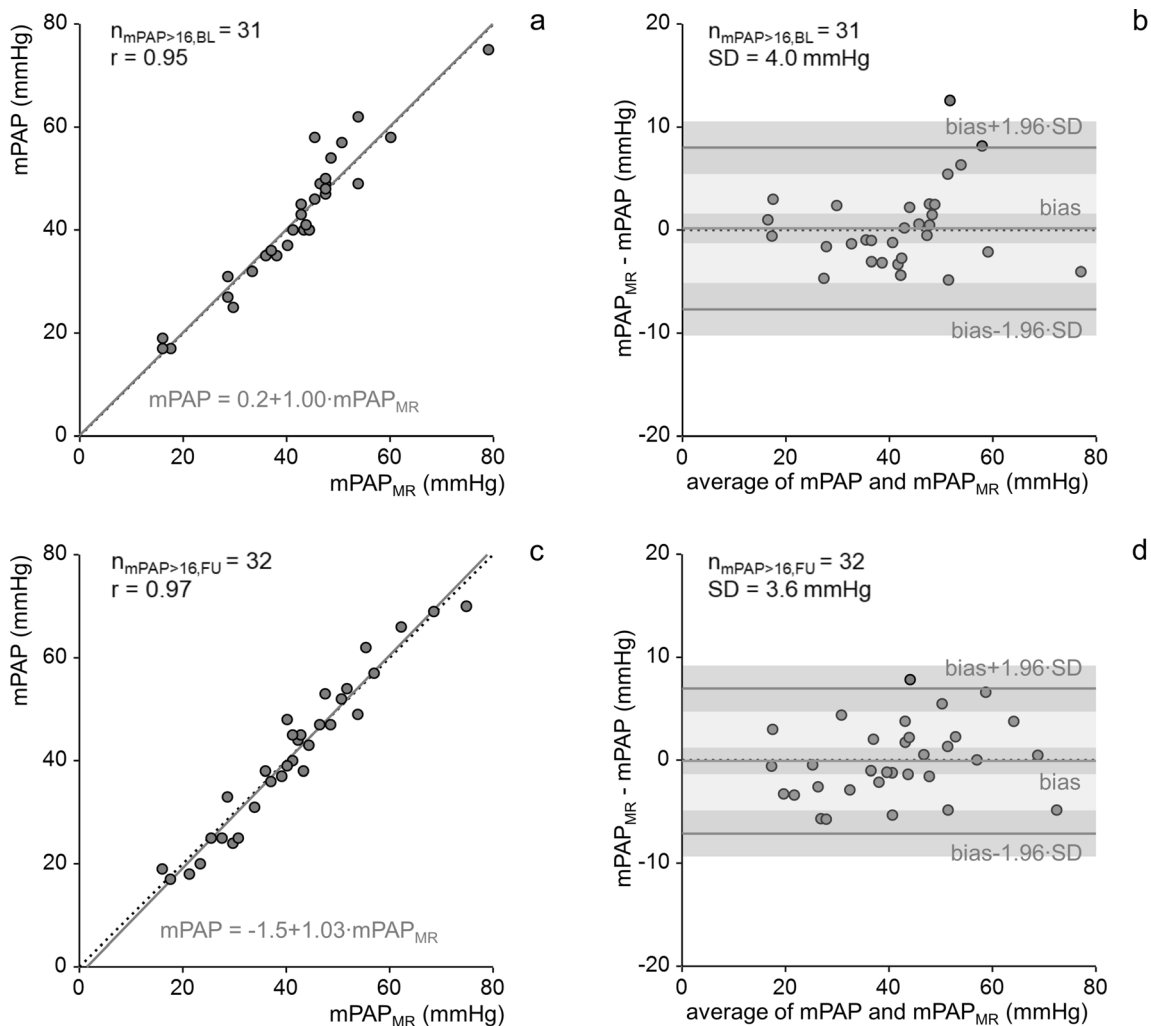
Fig. 4 Linear regression and Bland-Altman plots of mean pulmonary arterial pressures measured at right heart catheterization (mPAP) and estimated from vortex duration (mPAP$_{MR}$) at baseline (**a**, **b**) and follow-up (**c**, **d**). Light gray shading indicates the area between 95% limits of agreement, dark gray shadings indicate 95% confidence intervals of bias and 95%-limits of agreement. $n_{mPAP > 16,BL}$, number of subjects with mPAP > 16 mmHg at baseline; $n_{mPAP > 16,FU}$, number of subjects with mPAP > 16 mmHg at follow-up; r, correlation coefficient

allows both accurate prediction of the direction of mPAP changes and precise, non-invasive estimation of the magnitude of mPAP changes in patients with mPAP > 16 mmHg.

Stabilization and improvement of pulmonary hemodynamics are major objectives in the management of patients with PH [3, 32]. Doppler echocardiography is currently the primary non-invasive method for the evaluation of RV function and pulmonary arterial pressure during PH therapy [6, 24]. The technique, however, has limitations with respect to reproducibility [5, 33–37] and the accuracy of pulmonary arterial pressure estimation [36–39], potentially limiting the reliability of echocardiography for serial assessments of individual patients. Cardiac MRI has increasingly been used in PH studies as a reference standard for the evaluation of ventricular function [40–43]. These studies have identified progressive RV dilatation and decreased RV EF at follow-up cardiac MRI as important predictors of

poor long-term outcome and treatment failure. Moreover, van de Veerdonk et al [41] reported increasing RV volumes and decreased RV EF as early signs of clinical worsening in a group of severe PAH patients, suggesting that RV remodeling may precede disease progression even in patients appearing clinically stable. Notably, significant correlations were also found between RV ESV, RV EF, and RV SV changes and ΔmPAP in the present study.

Even though various routine cardiac MRI parameters and parameter models have been used for the evaluation of mPAP in PH showing their potential of mPAP prediction with standard deviations in the range of 7–10 mmHg [8, 12, 44], cardiac MRI is not yet established as a tool for the non-invasive estimation of mPAP. Reiter et al [27] demonstrated a more accurate 4D flow-based estimation of mPAP > 16 mmHg and high accuracy in the diagnosis of PH from the duration of vortical blood flow in the main
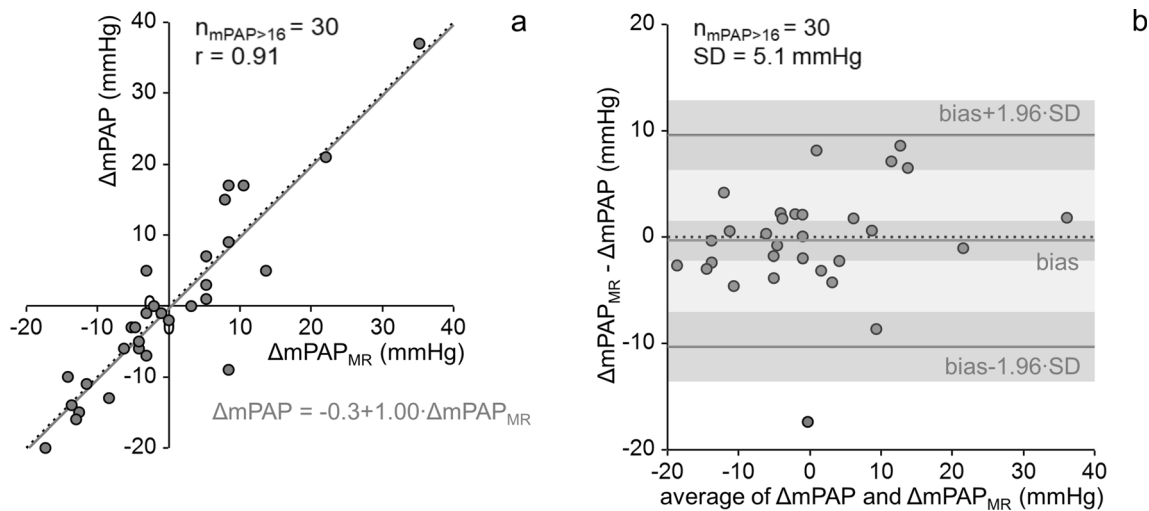
Fig. 5 Linear regression (**a**) and Bland-Altman (**b**) plot of mean pulmonary arterial pressure differences between baseline and follow-up measured by right heart catheterization (ΔmPAP). Light gray shading indicates the area between 95% limits of agreement, dark gray shadings indicate 95% confidence intervals of bias and 95% limits of agreement. $n_{mPAP > 16}$, number of subjects with mPAP > 16 mmHg at baseline and follow-up

pulmonary artery using a threshold of mPAP $\geq$ 25 mmHg, irrespective of the etiology of PH. Employed with the recently introduced threshold of mPAP > 20 mmHg for the diagnosis of PH [1] in the present study, the technique revealed the accuracy for the non-invasive diagnosis of PH similar to that which it yielded with the former threshold mPAP $\geq$ 25 mmHg [26–28]. Using a piecewise linear model for non-invasive estimation of mPAP > 16 mmHg [27], mPAP was—in accordance with [27, 28]—predicted without bias and with small standard deviations from RHC at baseline as well as follow-up cardiac MRI. As the differences between mPAP$_{MR}$ and mPAP did not depend on field strength and a main difference in 4D flow protocols at different field strength was the measured temporal resolution, it could be speculated that the measured temporal resolution of the 4D flow acquisition does not play a central role for the accuracy of mPAP estimation.

The standard deviation for the prediction of pressure differences in the present study was lower than anticipated by the law of error propagation, which would result in a standard deviation of $\sqrt{3.6^2 + 4.0^2} = 5.4$ mmHg. This can be understood to be due to the comparative interpretation of vortical blood flow along the main pulmonary artery observed at baseline and follow-up, which increases the likelihood that a combined over- or underestimation of vortex duration-derived mPAP at baseline and follow-up will be canceled out in the difference (ΔmPAP$_{MR}$). The standard deviation between invasively measured and non-invasively estimated ΔmPAP, however, cannot be expected to be substantially smaller than 5 mmHg, because RHC and MRI measurements were not acquired simultaneously: Assuming a spontaneous mPAP variability of

approximately 3 mmHg [26, 45, 46], deviations between RHC and MRI of at least $\sqrt{3^2 + 3^2} = 4.2$ mmHg have to be expected, even without taking into account the limited time resolution of vortex duration assessment.

The high accuracy for the prediction of mPAP increases and decreases in PH patients can be interpreted as a natural consequence of the strong correlation between ΔmPAP from RHC and MR. Considering mPAP changes within the range mPAP $\leq$ 16 mmHg as clinically not relevant (that is—as defined in the present study—no mPAP change), the accuracy of predicted mPAP changes in the whole population was comparable to that in the PH group. This result implies that the absence of vortical blood flow along the main pulmonary artery at baseline and follow-up in patients at risk of developing PH indicates persistent normal mPAP $\leq$ 16 mmHg [47].

Several limitations of the current study need to be acknowledged. As this was a retrospective analysis of two prospective studies, follow-up of patients was not planned and the follow-up times varied between 1 and 10 years. No patients with PH due to left heart diseases were included in the data analysis, as these patients were not repeatedly followed up by RHC. The study population included patients across a wide mPAP range, which limits the comparability of differences in the diagnosis of PH from the duration of vortical blood flow in the main pulmonary artery based on different mPAP cutoffs for PH. Moreover, only adult patients were recruited. Although protocols used for the assessment of 4D flow at 1.5 T and 3 T MRI differed, the bias of resulting pressure differences to RHC did not differ, indicating that results were not directly affected by the acquisition strategy.

In conclusion, MR 4D flow imaging allows accurate non-invasive prediction and quantification of mPAP changes in adult patients with PH or at risk of developing PH.

Compliance with ethical standards

Guarantor The scientific guarantor of this publication is Ursula Reiter.

Conflict of interest The authors of this manuscript declare relationships with the following companies: Gert Reiter is an employee of Siemens Healthcare Diagnostics GmbH, Austria. The study was performed under a Master Research Agreement between the Medical University of Graz, Graz University of Technology, and Siemens Healthcare Diagnostics GmbH.

The other authors of this manuscript declare no relationships with any companies whose products or services may be related to the subject matter of the article.

Statistics and biometry One of the authors (Gert Reiter) has significant statistical expertise. No complex statistical methods were necessary for this paper.

Informed consent Written informed consent was obtained from all patients in this study.

Ethical approval Institutional Review Board approval was obtained. Ethical committee: Medical University of Graz, Austria. ClinicalTrials.gov: NCT00575692 and NCT01725763

Study subjects or cohorts overlap Study patients were participants in two prospective studies enrolling consecutive patients with PH or with a risk of having PH and referring them for comprehensive cardiac MR imaging at 1.5 T and 3 T after RHC. Multiple studies have been published from these cohorts (Ref. 10, 26–28). This is the first study including 4D flow data from 3 T (NCT01725763), as well as follow-up 4D flow data at 1.5 T (NCT00575692).

Methodology
• retrospective analysis of two prospective studies
• diagnostic or prognostic study
• performed at one institution

References

1. Simonneau G, Montani D, Celermajer DS et al (2019) Haemodynamic definitions and updated clinical classification of pulmonary hypertension. Eur Respir J 53:1801913. https://doi.org/10.1183/13993003.01913-2018

2. Galiè N, Humbert M, Vachiery J-L et al (2016) 2015 ESC/ERS Guidelines for the diagnosis and treatment of pulmonary hypertension: The Joint Task Force for the Diagnosis and Treatment of Pulmonary Hypertension of the European Society of Cardiology (ESC) and the European Respiratory Society (ERS) Endorsed by: Association for European Paediatric and Congenital Cardiology (AEPC), International Society for Heart and Lung Transplantation (ISHLT). Eur Heart J 37:67–119. https://doi.org/10.1093/eurheartj/ehv317

3. McLaughlin VV, Gaine SP, Howard LS et al (2013) Treatment goals of pulmonary hypertension. J Am Coll Cardiol 62:D73–D81. https://doi.org/10.1016/j.jacc.2013.10.034

4. Wright LM, Dwyer N, Celermajer D, Kritharides L, Marwick TH (2016) Follow-Up of Pulmonary Hypertension With Echocardiography. JACC Cardiovasc Imaging 9:733–746. https://doi.org/10.1016/j.jcmg.2016.02.022

5. Sato T, Tsujino I, Ohira H et al (2017) Accuracy of echocardiographic indices for serial monitoring of right ventricular systolic function in patients with precapillary pulmonary hypertension. PLoS One 12:e0187806. https://doi.org/10.1371/journal.pone.0187806

6. Kiely DG, Levin DL, Hassoun PM et al (2019) Statement on imaging and pulmonary hypertension from the Pulmonary Vascular Research Institute (PVRI). Pulm Circ 9:204589401984199. https://doi.org/10.1177/2045894019841990

7. Swift AJ, Rajaram S, Condliffe R et al (2012) Diagnostic accuracy of cardiovascular magnetic resonance imaging of right ventricular morphology and function in the assessment of suspected pulmonary hypertension results from the ASPIRE registry. J Cardiovasc Magn Reson 14:40. https://doi.org/10.1186/1532-429X-14-40

8. Swift AJ, Rajaram S, Hurdman J et al (2013) Noninvasive estimation of PA pressure, flow, and resistance with CMR imaging. JACC Cardiovasc Imaging 6:1036–1047. https://doi.org/10.1016/j.jcmg.2013.01.013

9. Roller FC, Kriechbaum S, Breithecker A et al (2019) Correlation of native T1 mapping with right ventricular function and pulmonary haemodynamics in patients with chronic thromboembolic pulmonary hypertension before and after balloon pulmonary angioplasty. Eur Radiol 29:1565–1573. https://doi.org/10.1007/s00330-018-5702-x

10. Reiter U, Reiter G, Kovacs G et al (2017) Native myocardial T1 mapping in pulmonary hypertension: correlations with cardiac function and hemodynamics. Eur Radiol 27:157–166. https://doi.org/10.1007/s00330-016-4360-0

11. Swift AJ, Wild JM, Nagle SK et al (2014) Quantitative magnetic resonance imaging of pulmonary hypertension: a practical approach to the current state of the art. J Thorac Imaging 29:68–79. https://doi.org/10.1097/RTI.0000000000000079

12. Johns CS, Rajaram S, Capener DA et al (2018) Non-invasive methods for estimating mPAP in COPD using cardiovascular magnetic resonance imaging. Eur Radiol 28:1438–1448. https://doi.org/10.1007/s00330-017-5143-y

13. Johns CS, Kiely DG, Rajaram S et al (2019) Diagnosis of pulmonary hypertension with cardiac MRI: derivation and validation of regression models. Radiology 290:61–68. https://doi.org/10.1148/radiol.2018180603

14. Dellegrottaglie S, Sanz J, Poon M et al (2007) Pulmonary hypertension: accuracy of detection with left ventricular septal-to–free

wall curvature ratio measured at cardiac MR. Radiology 243:63–69. https://doi.org/10.1148/radiol.2431060067

15. Moral S, Fernández-Friera L, Stevens G et al (2012) New index alpha improves detection of pulmonary hypertension in comparison with other cardiac magnetic resonance indices. Int J Cardiol 161:25–30. https://doi.org/10.1016/j.ijcard.2011.04.024

16. Bradlow WM, Assomull R, Kilner PJ, Gibbs JS, Sheppard MN, Mohiaddin RH (2010) Understanding late gadolinium enhancement in pulmonary hypertension. Circ Cardiovasc Imaging 3:501–503. https://doi.org/10.1161/CIRCIMAGING.109.919779

17. Kreitner K-F, Wirth GM, Krummenauer F et al (2013) Noninvasive assessment of pulmonary hemodynamics in patients with chronic thromboembolic pulmonary hypertension by high temporal resolution phase-contrast MRI: correlation with simultaneous invasive pressure recordings*. Circ Cardiovasc Imaging 6:722–729. https://doi.org/10.1161/CIRCIMAGING.112.000276

18. Helderman F, Mauritz G-J, Andringa KE, Vonk-Noordegraaf A, Marcus JT (2011) Early onset of retrograde flow in the main pulmonary artery is a characteristic of pulmonary arterial hypertension. J Magn Reson Imaging 33:1362–1368. https://doi.org/10.1002/jmri.22581

19. Sieren MM, Berlin C, Oechtering TH et al (2019) Comparison of 4D Flow MRI to 2D Flow MRI in the pulmonary arteries in healthy volunteers and patients with pulmonary hypertension. PLoS One 14:e0224121. https://doi.org/10.1371/journal.pone.0224121

20. Mousseaux E, Tasu JP, Jolivet O, Simonneau G, Bittoun J, Gaux JC (1999) Pulmonary arterial resistance: noninvasive measurement with indexes of pulmonary flow estimated at velocity-encoded mr imaging—preliminary experience. Radiology 212:896–902. https://doi.org/10.1148/radiology.212.3.r99au21896

21. Hosokawa K, Abe K, Horimoto K, Yamasaki Y, Nagao M, Tsutsui H (2018) Balloon pulmonary angioplasty relieves haemodynamic stress towards untreated-side pulmonary vasculature and improves its resistance in patients with chronic thromboembolic pulmonary hypertension. EuroIntervention 13:2069–2076. https://doi.org/10.4244/EIJ-D-17-00888

22. Odagiri K, Inui N, Hakamata A et al (2016) Non-invasive evaluation of pulmonary arterial blood flow and wall shear stress in pulmonary arterial hypertension with 3D phase contrast magnetic resonance imaging. Springerplus 5:1071. https://doi.org/10.1186/s40064-016-2755-7

23. Roldán-Alzate A, Frydrychowicz A, Johnson KM et al (2014) Non-invasive assessment of cardiac function and pulmonary vascular resistance in an canine model of acute thromboembolic pulmonary hypertension using 4D flow cardiovascular magnetic resonance. J Cardiovasc Magn Reson 16:23. https://doi.org/10.1186/1532-429X-16-23

24. Rengier F, Melzig C, Derlin T, Marra AM, Vogel-Claussen J (2019) Advanced imaging in pulmonary hypertension: emerging techniques and applications. Int J Cardiovasc Imaging 35:1407–1420. https://doi.org/10.1007/s10554-018-1448-4

25. Han QJ, Witschey WRT, Fang-Yen CM et al (2015) Altered right ventricular kinetic energy work density and viscous energy dissipation in patients with pulmonary arterial hypertension: a pilot study using 4D flow MRI. PLoS One 10:e0138365. https://doi.org/10.1371/journal.pone.0138365

26. Reiter G, Reiter U, Kovacs G et al (2008) Magnetic resonance–derived 3-dimensional blood flow patterns in the main pulmonary artery as a marker of pulmonary hypertension and a measure of elevated mean pulmonary arterial pressure. Circ Cardiovasc Imaging 1:23–30. https://doi.org/10.1161/CIRCIMAGING.108.780247

27. Reiter G, Reiter U, Kovacs G, Olschewski H, Fuchsjäger M (2015) Blood flow vortices along the main pulmonary artery measured with MR imaging for diagnosis of pulmonary hypertension. Radiology 275:71–79. https://doi.org/10.1148/radiol.14140849

28. Reiter U, Reiter G, Kovacs G et al (2013) Evaluation of elevated mean pulmonary arterial pressure based on magnetic resonance 4D velocity mapping: comparison of visualization techniques. PLoS One 8:e82212. https://doi.org/10.1371/journal.pone.0082212

29. Ota H, Sugimura K, Miura M, Shimokawa H (2015) Four-dimensional flow magnetic resonance imaging visualizes drastic change in vortex flow in the main pulmonary artery after percutaneous transluminal pulmonary angioplasty in a patient with chronic thromboembolic pulmonary hypertension. Eur Heart J 36:1630–1630. https://doi.org/10.1093/eurheartj/ehv054

30. Han QJ, Contijoch F, Forfia PR, Han Y (2016) Four-dimensional flow magnetic resonance imaging visualizes drastic changes in the blood flow in a patient with chronic thromboembolic pulmonary hypertension after pulmonary thromboendarterectomy. Eur Heart J 37:2802–2802. https://doi.org/10.1093/eurheartj/ehw064

31. Gulsun Mehmet A, Jolly M-P, Guehring J et al (2012) A novel 4D flow tool for comprehensive blood flow analysis. Proc Intl Soc Mag Reson Med, Melbourne, p 1176

32. McLaughlin VV, Shah SJ, Souza R, Humbert M (2015) Management of pulmonary arterial hypertension. J Am Coll Cardiol 65:1976–1997. https://doi.org/10.1016/j.jacc.2015.03.540

33. Amsallem M, Sternbach JM, Adigopula S et al (2016) Addressing the controversy of estimating pulmonary arterial pressure by echocardiography. J Am Soc Echocardiogr 29:93–102. https://doi.org/10.1016/j.echo.2015.11.001

34. Choi JH, Joo S-J, Kim J (2016) Determining the necessity for right heart catheterization in pulmonary hypertension associated with connective tissue diseases assessed by echocardiography. Int J Rheum Dis 19:65–73. https://doi.org/10.1111/1756-185X.12769

35. Spruijt OA, Di Pasqua MC, Bogaard HJ et al (2017) Serial assessment of right ventricular systolic function in patients with precapillary pulmonary hypertension using simple echocardiographic parameters: a comparison with cardiac magnetic resonance imaging. J Cardiol 69:182–188. https://doi.org/10.1016/j.jjcc.2016.02.019

36. Finkelhor RS, Lewis SA, Pillai D (2015) Limitations and strengths of Doppler/echo pulmonary artery systolic pressure-right heart catheterization correlations: a systematic literature review. Echocardiography 32:10–18. https://doi.org/10.1111/echo.12594

37. Fisher MR, Forfia PR, Chamera E et al (2009) Accuracy of Doppler echocardiography in the hemodynamic assessment of pulmonary hypertension. Am J Respir Crit Care Med 179:615–621. https://doi.org/10.1164/rccm.200811-1691OC

38. Taleb M, Khuder S, Tinkel J, Khouri SJ (2013) The diagnostic accuracy of Doppler echocardiography in assessment of pulmonary artery systolic pressure: a meta-analysis. Echocardiography 30:258–265. https://doi.org/10.1111/echo.12061

39. Ni J-R, Yan P-J, Liu S-D et al (2019) Diagnostic accuracy of transthoracic echocardiography for pulmonary hypertension: a systematic review and meta-analysis. BMJ Open 9:e033084. https://doi.org/10.1136/bmjopen-2019-033084

40. van Wolferen SA, Marcus JT, Boonstra A et al (2007) Prognostic value of right ventricular mass, volume, and function in idiopathic pulmonary arterial hypertension. Eur Heart J 28:1250–1257. https://doi.org/10.1093/eurheartj/ehl477

41. van de Veerdonk MC, Marcus JT, Westerhof N et al (2015) Signs of right ventricular deterioration in clinically stable patients with pulmonary arterial hypertension. Chest 147:1063–1071. https://doi.org/10.1378/chest.14-0701

42. van de Veerdonk MC, Kind T, Marcus JT et al (2011) Progressive right ventricular dysfunction in patients with pulmonary arterial hypertension responding to therapy. J Am Coll Cardiol 58:2511–2519. https://doi.org/10.1016/j.jacc.2011.06.068

43. Baggen VJM, Leiner T, Post MC et al (2016) Cardiac magnetic resonance findings predicting mortality in patients with pulmonary arterial hypertension: a systematic review and meta-analysis. Eur Radiol 26:3771–3780. https://doi.org/10.1007/s00330-016-4217-6

44. Zhang Z, Wang M, Yang Z et al (2017) Noninvasive prediction of pulmonary artery pressure and vascular resistance by using cardiac magnetic resonance indices. Int J Cardiol 227:915–922. https://doi.org/10.1016/j.ijcard.2016.10.068

45. Rich S, D'alonzo GE, Dantzker DR, Levy PS (1985) Magnitude and implications of spontaneous hemodynamic variability in primary pulmonary hypertension. Am J Cardiol 55:159–163. https://doi.org/10.1016/0002-9149(85)90319-4

46. Mehmood M, Agarwal R, Raina A, Correa-Jaque P, Benza RL (2016) Hemodynamic response to treatment of iron deficiency anemia in pulmonary arterial hypertension: longitudinal insights from an implantable hemodynamic monitor. Pulm Circ 6:616–618. https://doi.org/10.1086/688670

47. Kovacs G, Berghold A, Scheidl S, Olschewski H (2009) Pulmonary arterial pressure during rest and exercise in healthy subjects: a systematic review. Eur Respir J 34:888–894. https://doi.org/10.1183/09031936.00145608